PHYSICAL REVIEW B **86**, 140104(R) (2012)

Evidence of nanoscale structural phase separation in large bandwidth $La_{0.2}Sr_{0.8}MnO_3$

R. Bindu,[1,*] Sanjay Singh,[2] Navneet Singh,[1] Rajeev Ranjan,[3] Kalobaran Maiti,[4] A. H. Hill,[5,†] and S. R. Barman[2]

[1]*School of Basic Sciences, Indian Institute of Technology Mandi, Mandi, Himachal Pradesh 175001, India*

[2]*UGC-DAE Consortium for Scientific Research, Khandwa Road, Indore 452001, India*

[3]*Department of Materials Engineering, Indian Institute of Science, Bangalore 560012, India*

[4]*Department of Condensed Matter Physics and Materials Science, Tata Institute of Fundamental Research, Homi Bhabha Road, Colaba, Mumbai 400005, India*

[5]*European Synchrotron Radiation Facility, 6 rue Jules Horowitz, F-38000 Grenoble, France*

(Received 3 September 2012; published 19 October 2012)

We have investigated the structural evolution of $La_{0.2}Sr_{0.8}MnO_3$ using temperature dependent high resolution synchrotron x-ray diffraction technique. In a wide temperature range, $La_{0.2}Sr_{0.8}MnO_3$ reveals nanoscale structural inhomogeneity consisting of cubic and tetragonal phases. The present results suggest that domains of nanometer size of the tetragonal (low temperature) phase start nucleating in the cubic (high temperature) phase even above the Néel temperature (T_N). The tetragonal phase fraction increases substantially below T_N. Detailed analysis suggests that the twinned phase is tetragonal, orbital ordered, and insulating. At temperatures below 170 K, a small amount of the cubic phase is retained. The present results reveal the significance of the connectivity between the nanoscale structural phase separation with the physical properties.

DOI: 10.1103/PhysRevB.86.140104 PACS number(s): 64.75.Jk, 61.05.cp, 71.27.+a, 75.47.Lx

Strongly correlated electron systems show many exotic behaviors due to strong coupling between charge, spin, orbital, and lattice degrees of freedom.[1] One interesting phenomenon in the condensed matter physics is the observation of charge ordering in many mixed valence transition metal oxides,[2] which often leads to insulating phases due to localization of charge carriers.[1,2] The existence of charge ordering in the metallic phase is a rare event, although such a possibility has been predicted theoretically.[3] The observation of linear specific heat at low temperature in the nonmetallic systems is another fascinating physical phenomenon, which has been attracting the attention of researchers for a significant period.[4] Such behavior was observed in the amorphous systems and this was understood by the tunneling model proposed by Anderson*et al*.[5] In the case of manganites, both the above mentioned physical phenomena are ubiquitous.[6] The occurrence of charge ordering and resulting insulating behavior are so widely observed that the jump in the resistivity has often been attributed to the signature of charge ordering.[1,2]

$La_{0.2}Sr_{0.8}MnO_3$ is cubic and metallic at room temperature (RT). It undergoes electronic and magnetic transitions from metal to insulator and paramagnetic to C-type antiferromagnetic at $\sim T_N = 265$ K.[7–12] In addition, it exhibits a jump in resistivity that can be attributed to a possible signature of charge ordering. However, recent transmission electron microscopy (TEM) studies have revealed the signature of charge ordering significantly above T_N.[10] Interestingly, it shows the coexistence of two phases, charge ordered cubic with an unidentified crystal structure of a twinned phase in the temperature range 260 K to 98 K. On cooling the sample, the twinned phase appears to grow at the cost of the charge ordered phase and is associated with the resistivity behavior.[10] High resolution photoemission results revealed finite density of states even in the insulating phase below T_N. A hard gap was observed only below 200 K. Ironically, the specific heat exhibits a linear dependence with temperature below 10 K in this insulating phase.[11,12] Evidently, the system is complex, with a plethora of unresolved fundamental issues such as the observation of linear specific heat in a gapped phase, existence of charge ordering in the insulating phase, the nature of metal to insulator transition at T_N, etc. Probing the connectivity between the phase coexistence and physical properties requires quantitative information about the phase fractions and its gradual thermal evolution.

Thus we employed high resolution synchrotron x-ray diffraction studies on $La_{0.2}Sr_{0.8}MnO_3$ as a function of temperature. The advantages of this technique are that one can achieve ultrahigh resolution and extract quantitative information of the phase fractions. Our results show a signature of the domains of the tetragonal phase in the matrix of cubic phase for temperatures well above RT whose sizes above 250 K are too small to be manifested as a distinct peak in the diffraction patterns. In the temperature range 250 to 170 K, distinct peaks related to the tetragonal phase are observed and its fraction grows at the cost of the cubic phase. Our studies have shown the twinned tetragonal phase is orbital ordered and insulating. For $T < 170$ K, the fraction of the cubic charged ordered phase remains unaltered. The significance of these results in understanding the various physical properties has also been discussed.

Synchrotron x-ray diffraction measurements were performed on the high-resolution powder diffractometer ID31 at the ESRF, Grenoble. The powder sample was sealed in a borosilicate capillary and data were recorded for twelve different temperatures in the range 300–90 K with wavelength of $\lambda = 0.399\,93$ Å. The beam is monochromated by a cooled double-crystal monochromator. The capillary was spun on the axis of the diffractometer to reduce any preferred orientation and packing effects. A bank of nine detectors is scanned vertically to measure the diffracted intensity as a function of 2θ. Each detector is preceded by a Si(111) analyzer crystal and the detector channels are approximately 2° apart. The instrumental contribution to the full width at half maximum (FWHM) is around $2\theta = 0.003^\circ$.

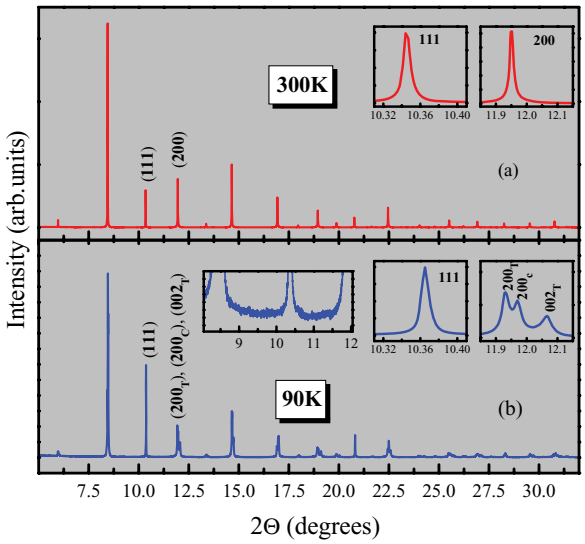

FIG. 1. (Color online) Synchrotron x-ray powder diffraction patterns of $La_{0.2}Sr_{0.8}MnO_3$ at 300 K and 90 K. The Bragg peaks (*111*), (*200*) in the cubic and tetragonal phases are shown in the insets (a) and (b), respectively. The inset (b) also contains the pattern in the expanded scale in the angular region 8° to 12°.

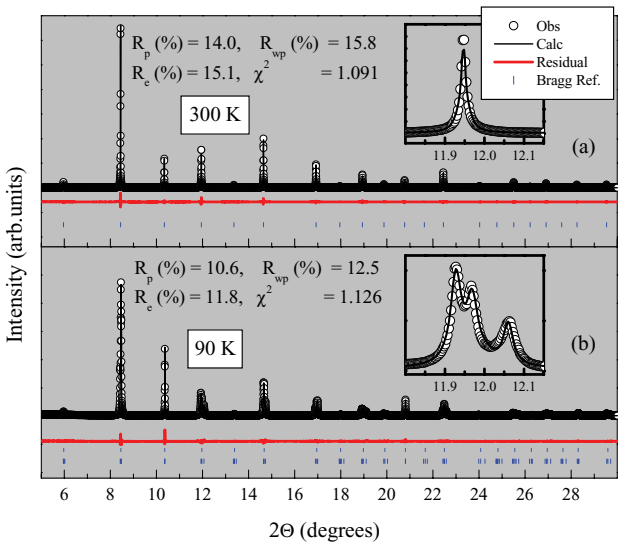

FIG. 2. (Color online) Typical Rietveld fittings of the x-ray diffraction patterns for 300 K and 90 K. The open circle and the solid line correspond to the observed and calculated patterns, respectively. The difference pattern is given by the line below the experimental patterns. The vertical bars correspond to the Bragg reflections. R_p, R_{wp}, R_e, and χ^2 correspond to the profile, weighted profile, the expected weighted profile factors, and the reduced chi-square, respectively. The magnified view of the fit in the angular range 11.8° to 12.15° is shown in the inset.

Significant changes in the Bragg profiles of x-ray powder diffraction patterns of $La_{0.2}Sr_{0.8}MnO_3$ occur as the sample is cooled from 300 K to 90 K (Fig. 1). The peaks are indexed using the FULLPROF Rietveld profile refinement software.[13,14] All the peaks at RT correspond to the cubic phase with space group $Pm\bar{3}m$ consistent with our finding in earlier studies.[11] At 90 K, except for the cubic (*hhh*) Bragg profiles, the peaks appear as multiplets. For example, the (*200*) cubic peak appears to be split into a triplet at 90 K, while the (*111*) remains as singlet—this is shown with clarity in the inset of Fig. 1(b). Detailed analysis reveals that the pattern at 90 K can be indexed with coexisting cubic and tetragonal structural models. As shown in the right inset of Fig. 1(b), the triplet corresponds to two tetragonal reflections (200_T) and (002_T) and one cubic reflection (200_C). The singlet nature of (*111*) peak at 90 K implies identical values of d_{111} for both the phases. Thus the gradual cubic to tetragonal transformation occurs in such a way as to preserve the integrity of the (*111*) plane, which can be considered as the invariant plane of this transformation.

In general most of the noncubic perovskites possess octahedral tilts giving rise to superlattice reflections in the diffraction pattern.[15] For example, the parent compound, $LaMnO_3$, has octahedral structure (space group *Pbnm*) with octahedral tilts conventionally designated as $a^-a^-c^+$ in Glazer's notation.[15] The two possible octahedral tilts, $a^0a^0c^+$ and $a^0a^0c^-$, compatible with the tetragonal distortion of the cubic lattice, is expected to give rise to superlattice reflections at $2\Theta \sim 9.5°$ and 9.9°, respectively. However, as is evident from the left inset of Fig. 1(b), no trace of extra peaks could be observed in this angular region of the diffraction pattern. The tetragonal structure therefore does not consist of an octahedral tilt. This implies that, as in the cubic phase, all the Mn-O-Mn angles in the tetragonal phase are either 90° or 180°. The most symmetric space group consistent with this tetragonal structure was found to be *P4/mmm*. Rietveld profile refinement of the 90 K pattern was accordingly carried out using $Pm\bar{3}m$ and *P4/mmm* phase coexistence model. The good quality of the Rietveld fit shown in Fig. 2 confirms this choice of structural model at 90 K.

The variation of the cubic phase fraction as a function of temperature is shown in Fig. 3(a). Just below T_N, the cubic phase fraction decreases drastically from about 79% at 250 K to about 9% at 150 K. Below 170 K, the phase fractions remain almost unchanged down to 90 K. The temperature variation of the cubic and tetragonal lattice parameters are shown in Fig. 3(b). In the cubic phase, the lattice parameter gradually decreases with decreasing temperature that can be attributed to the thermal contraction. But for the tetragonal phase, it shows a decrement in the c parameter and a corresponding increment in the a parameter. With a further decrease in the temperature, there is no significant change seen in the lattice parameter a whereas the lattice parameter c decreases. The unit cell volume exhibits a continuous decrease with decrease in temperature in both cases. The unit cell volume for the tetragonal phase appearing below T_N is found to be less than the value of the cubic phase as shown in Fig. 3(c). Thus there is a discontinuous change in the unit cell volume, Fig. 3(c), which suggests that the structural transition is first order in nature. The behavior of the lattice parameters in the tetragonal phase where $c < a$ may be related to the coupling between the electronic and lattice degrees of freedom. In the octahedral crystal field, the Mn 3*d* levels split into triply degenerate, t_{2g}, and doubly degenerate, e_g, bands. A compression along the z axis leads to further splitting of the bands—the doubly degenerate e_g band will split into two nondegenerate bands possessing b_{1g} and a_{2g} symmetry, with

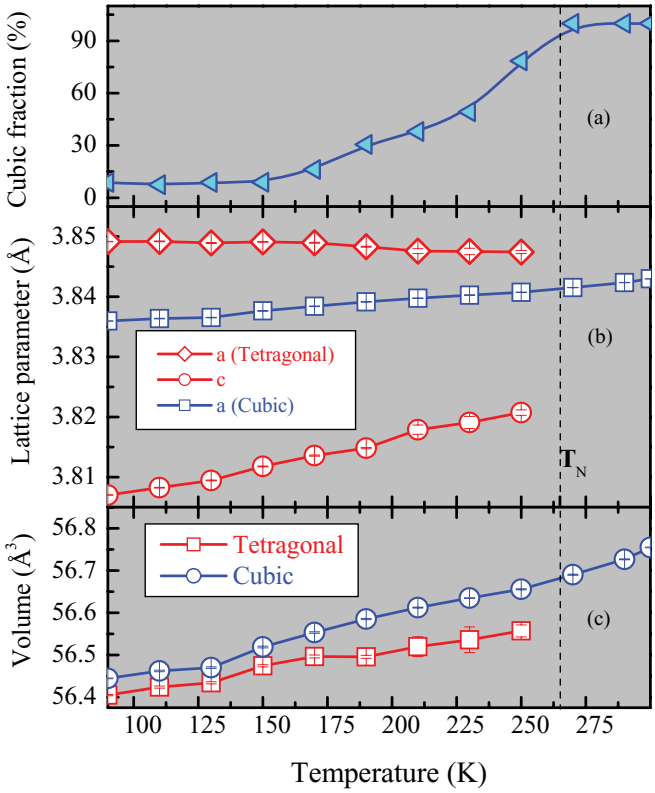

FIG. 3. (Color online) Temperature dependence of (a) cubic phase fraction and (b) lattice parameters. Open diamond and circle correspond to the tetragonal phase and open square corresponds to the cubic phase. The vertical line at 265 K marks the Néel temperature (T_N). The size of the symbols are equivalent to the error bars. (c) Unit cell volume of the cubic (open circle) and tetragonal (open square) phases.

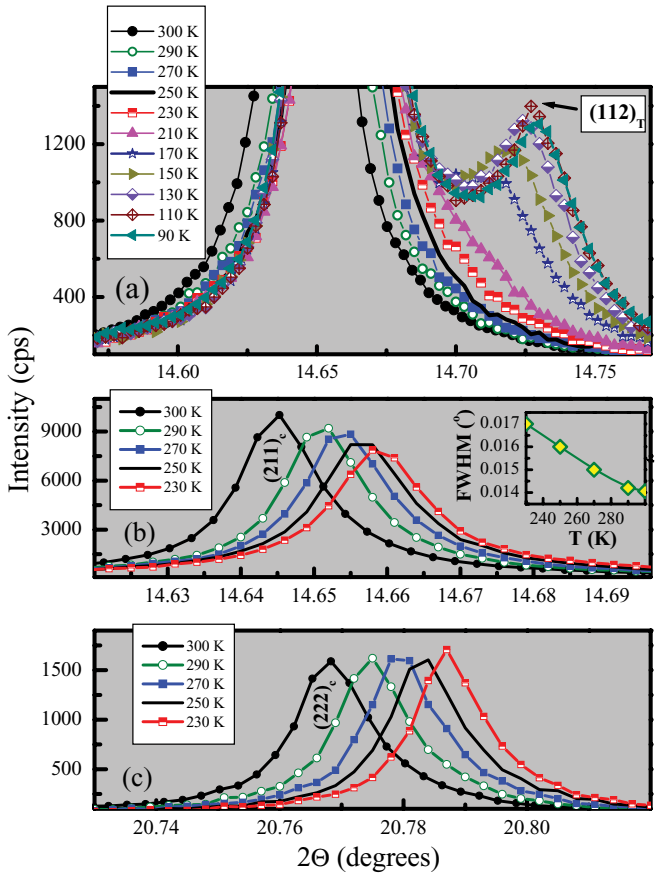

FIG. 4. (Color online) Temperature evolution of the intensity of (a) tetragonal Bragg peak in an expanded scale, (b) cubic (*211*) Bragg reflection, and (c) (*222*) Bragg reflection. The inset shows the behavior of the FWHM of (*211*) peak.

b_{1g} band consisting of $d_{x^2-y^2}$ orbital having lower energy. Mn^{3+} has four 3*d* electrons. Considering Hund's rule, three electrons will occupy the t_{2g} up spin band. In the presence of distortion, the fourth electron will occupy the $d_{x^2-y^2}$ band. Thus the longer *a* parameter as compared to the *c* parameter is indicative of the occupation of the electrons in the $d_{x^2-y^2}$ orbitals than the $d_{z^2-r^2}$ orbitals. Such preferential occupation of $d_{x^2-y^2}$ orbitals as compared to $d_{3z^2-r^2}$ and its cooperative behavior suggests orbital ordering. The above results suggest that orbital ordering may be responsible for the stabilization of the tetragonal phase. Such orbital ordering finally leads to superexchange interaction and stabilizes the material in the C-type antiferromagnetic phase. These interactions can be understood based on Goodenough and Kannamori's rule,[16] where the magnetic structure depends on the occupation of the neighboring e_g orbitals.

Here, we discuss the temperature evolution of a few representative Bragg profiles. On cooling, a weak tetragonal peak becomes barely visible at 250 K [Fig. 4(a)]. Interestingly, the peak heights of the Bragg reflections (*hkl*) continuously decrease on cooling even in the cubic phase [Fig. 4(b)]. In contrast, the height of the (*hhh*) peaks remain unaffected at all temperatures [Fig. 4(c)]. The temperature variation of the peak intensities of (*200*) and (*222*) cubic reflections is shown in Fig. 5(a). The systematic decrease in the intensity is possibly a manifestation of genuine structural changes taking place in the system at subnanometer length scale. The intensity lost at the peak position must be distributed between the peak and the tail region of the individual Bragg profiles. The gradual increase in the FWHM of a representative cubic (*211*) peak on cooling in the temperature range 300 to 230 K, shown in the inset of Fig. 4(b), confirms this point. It is most likely that the extra intensity away from the cubic Bragg peaks position is due to the scattering by the subnanometer sized nuclei of the tetragonal phase in the cubic matrix. It is interesting to note that the FWHM and peak count of the (*222*) reflection remain nearly unaffected in the entire temperature range. As mentioned above, this can be understood by the fact that the d_{hhh} of the cubic and tetragonal peaks are almost equal at all temperatures, even for the subnanometer sized tetragonal nuclei. Since, in general, it is well known that increase of temperature leads to decrease in the intensity of the Bragg reflections due to thermal diffuse scattering, the peak count in Fig. 5(a) is expected to exhibit a maximum somewhere above room temperature, i.e., when the system becomes free from the nuclei of the low temperature tetragonal phase. This implies that the coherently scattering domain size of the tetragonal phase remains small in the system, presumably due to high density of stable nuclei formed in the temperature region 300 to 250 K.

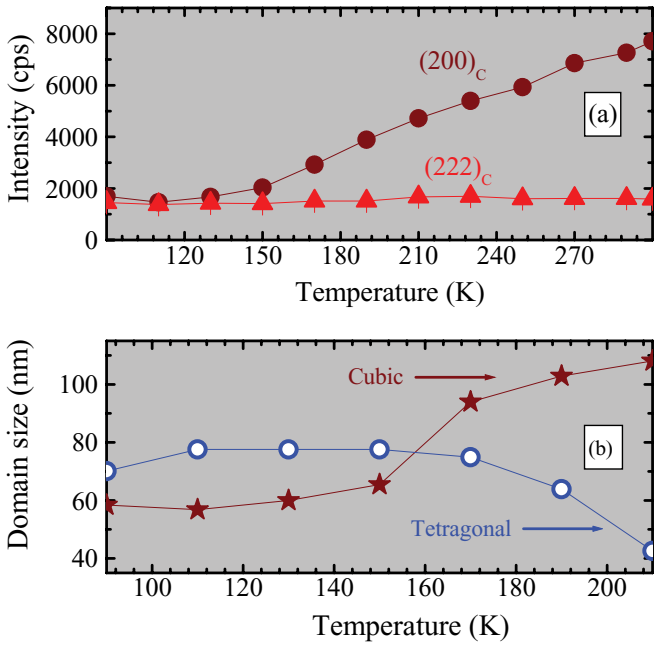

FIG. 5. (Color online) Temperature dependence of (a) the intensity of cubic (*200*) and (*222*) Bragg reflections and (b) the domain size of the tetragonal and cubic phase fractions.

These results clearly suggest that the pure cubic structure would exist somewhere above room temperature. On cooling the sample, the tetragonal phase starts nucleating in the cubic matrix, whose size keeps on growing with further reduction of temperature. Down to 230 K, the size of the nuclei of the tetragonal phase is not large enough to give the distinct diffraction patterns. The rough estimate of the domain size of the cubic and tetragonal phases were obtained by using the Scherrer formula and are shown in Fig. 5(b). At 300 K, because the average structure is cubic, the size obtained is the average grain size. At 210 K, the domain size of the cubic and tetragonal phases are found to be ∼108 and 43 nm, respectively. On reduction of temperature to 150 K, the domain size of the cubic phase decreases to ∼65 nm and that of the tetragonal phase increases to ∼78 nm. Further decrease of temperature below 150 K does not lead to any significant change in the domain size and phase fraction [Fig. 3(a)] of both the phases.

The present work unambiguously establishes the coexistence of two structural phases in a wide temperature region. It is expected that these two phases should have different electronic properties. At room temperature the compound is metallic and weakly charge ordered as revealed by our PES and TEM studies, respectively.[10,11] On reducing the temperature, the weak charge ordered phase becomes stronger and distinct superlattice peaks are evident at around 235 K. Around this temperature, finite spectral DOS (density of states) is also observed at the Fermi level where we found ∼50% cubic phase fractions. The hard gap only opened up below 200 K where the tetragonal phase fractions are more than 80%. These observations clearly suggest the insulating nature of the tetragonal phase and also appear to question the conventional existence of insulating behavior in the charge ordered region, which is cubic in our case.

Temperature dependent high resolution synchrotron x-ray diffraction studies have been carried out on $La_{0.2}Sr_{0.8}MnO_3$. Above the room temperature, the tetragonal phase starts nucleating in the matrix of the cubic phase. As the temperature is reduced, the competing fractions of the tetragonal phase grow in size at the cost of the cubic phase, although it is still possible to discern the former phase in the diffraction profiles for $T < 250$ K. Our detailed analysis has shown that the twinned tetragonal phase is orbital ordered and insulating and the cubic charge ordered phase gets frozen at low temperatures. The implications of these results in understanding the various physical properties have been discussed, which suggests that the physics of overdoped manganites cannot be understood within the homogenous picture. It appears that intrinsic inhomogeneity is a generic feature in similar such systems and further studies are required in this direction.

We thank A. Fitch, P. Rajput, J. Nayak, and A. Rai for useful discussions and experimental support. One of the authors, K.M., thanks the Department of Science and Technology, Govt. of India for financial assistance under Swarnajayanti Programme. S.R.B. and S.S. thank Max Planck Partner Group project for funding. N.S. thanks Ministry of Human Resource Development, India for the award of fellowship. S.S. thanks C.S.I.R., New Delhi for fellowship.

*Corresponding author: bindu@iitmandi.ac.in

†Present address: Johnson Matthey Technology Centre, Sonning Common, United Kingdom.

[1]T. V. Ramakrishnan, Curr. Sci. **95**, 1284 (2008); J. B. Goodenough, Rep. Prog. Phys. **67**, 1915 (2004); J. M. D. Coey and M. V. S. von Molnaacuter, Adv. Phys. **48**, 167 (1999); Y. Tokura, Phys. Today **56**, 50 (2003); *Colossal Magnetoresistance, Charge Ordering and Related Properties of Manganese Oxides*, edited by C. N. R. Rao and B. Raveau (World Scientific, Singapore, 1998); M. B. Salamon and M. Jaime, Rev. Mod. Phys. **73**, 583 (2001); E. Dagotto *et al.*, Phys. Rep. **344**, 1 (2001).

[2]E. J. W. Verwey, Nature (London) **144**, 327 (1939); E. J. W. Verway and P. W. Haayman, Physica **8**, 979 (1941); M. Isobe and Y. Ueda, J. Phys. Soc. Jpn. **65**, 1178 (1996); Y. Tokura, H. Kuwahara, Y. Moritomo, Y. Tomioka, and A. Asamitsu, Phys. Rev. Lett. **76**, 3184 (1996); J. P. Attfield, Solid State Sci. **8**, 861 (2006); M. Imada, A. Fujimori, and Y. Tokura, Rev. Mod. Phys. **70**, 1039 (1998).

[3]K. Hanasaki and M. Imada, J. Phys. Soc. Jpn. **74**, 2769 (2005).

[4]R. C. Zeller and R. O. Pohl, Phys. Rev. B **4**, 2029 (1971).

[5]P. W. Anderson *et al.*, Philos. Mag. **25**, 1 (1972).

[6]M. B. Salamon and M. Jaime, Rev. Mod. Phys. **73**, 583 (2001); A. Banerjee, R. Rawat, K. Mukherjee, and P. Chaddah, Phys. Rev. B **79**, 212403 (2009); L. Ghivelder, I. A. Castillo, M. A. Gusmao, J. A. Alonso, and L. F. Cohen, *ibid.* **60**, 12184 (1999).

[7]J. Hemberger, A. Krimmel, T. Kurz, H. A. KrugvonNidda, V. Y. Ivanov, A. A. Mukhin, A. M. Balbashov, and A. Loidl, Phys. Rev. B **66**, 094410 (2002).

[8]O. Chmaissem, B. Dabrowski, S. Kolesnik, J. Mais, J. D. Jorgensen, and S. Short, Phys. Rev. B **67**, 094431 (2003).

[9]F. Hiroyuki, F. Tetsuo, and I. Manabu, J. Phys. Soc. Jpn. **67**, 2582 (1998).

[10]R. Bindu, G. Adhikary, N. Sahadev, N. P. Lalla, and K. Maiti, Phys. Rev. B **84**, 052407 (2011).

[11]R. Bindu, G. Adhikary, S. K. Pandey, S. Patil, and K. Maiti, New J. Phys. **12**, 033003 (2010).

[12]R. Bindu, K. Maiti, R. Rawat, and S. Khalid, Appl. Phys. Lett. **92**, 121906 (2008).

[13]J. R. Carvajal, FULLPROF, a Rietveld refinement and pattern matching analysis program, Laboratoire Leon Brillouin, CEA-CNRS, France, 2000.

[14]H. M. Rietveld, Acta Crystallogr. **22**, 151 (1967); J. Appl. Cryst. **2**, 65 (1969); A. W. Hewat, Harwell Report No. 73/239 (1973), ILL Report No. 74/H62S (1974); G. Malmros and J. O. Thomas, J. Appl. Cryst. **10**, 7 (1977); C. P. Khattak and D. E. Cox, *ibid.* **10**, 405 (1977).

[15]A. M. Glazer, Acta Crystallogr. A **31**, 756 (1975); **28**, 3384 (1972).

[16]D. I. Khomskii, *Basic Aspects of Quantum Theory of Solids* (Cambridge University Press, Cambridge, UK, 2010).